JOURNAL OF CATALYSIS **172,** 34–45 (1997)
ARTICLE NO. CA971812

Cu–Na–ZSM-5 Catalysts Prepared by Chemical Transport: Investigations on the Role of Brønsted Acidity and of Excess Copper in the Selective Catalytic Reduction of NO by Propene

T. Liese and W. Grünert[1]

Lehrstuhl für Technische Chemie, Ruhr-Universität Bochum, D-44780 Bochum, Germany

Received November 6, 1996; revised April 1, 1997; accepted June 30, 1997

Cu–Na–ZSM-5 catalysts were prepared by a dry technique from physical mixtures of Na–ZSM-5 with copper compounds (CuCl, $Cu(NO_3)_2$ or $Cu(CH_3COO)_2$) in order to obtain intrazeolite copper species coexisting with the full amount of Na^+ ions of the parent zeolite. For this purpose, the parent mixtures were heated in inert gas or vacuum to 823–873 K. The transport of copper into the near-surface regions of the zeolite crystals was monitored by surface-analytical techniques (XPS, X-ray induced AES), into the bulk of the crystals by infrared spectroscopy of adsorbed pyridine. It was found that the chemical transport is most intense for copper associated with chlorine, but intrazeolite copper can be stabilized also in chlorine-free systems. When H–ZSM-5 is available together with Na–ZSM-5, solid-state ion exchange into the former predominates over chemical transport into the latter. The activity of these samples for the selective catalytic reduction of NO by propene was investigated in a broad temperature range and compared with the activity of reference catalysts prepared by aqueous exchange, which exhibited Brønsted acidity. Reaction rates normalized to the copper content were in the same order of magnitude for both types of Cu–ZSM-5 samples, which demonstrates the irrelevance of Brønsted acidity for the SCR by propene over Cu–ZSM-5. On the basis of surface-analytical data and trends in the temperature dependence of the activity, it was suggested that both isolated copper ions and intrazeolite but extralattice copper oxide clusters provide active sites for the SCR reaction.

INTRODUCTION

Following its first description by Iwamoto *et al.* (1) and Held *et al.* (2), the selective catalytic reduction of NO by hydrocarbons (SCR-HC) has been studied with a variety of catalytic systems and hydrocarbon reductants (3–5) without having been included so far into a commercial exhaust gas purification unit neither for mobile nor for stationary sources. In this situation, the knowledge of the catalytic reaction mechanism and of the functions that a successful catalyst must provide is of prime importance for the development of improved catalytic materials. Even for the well-studied Cu–ZSM-5 system, there are still many controversial questions, among them the nature of the active copper species and the role of Brønsted acidity in the reaction mechanism.

Brønsted acidity has been considered an essential feature of a good catalyst since the early days of SCR-HC. This is inferred by the superiority of alkene reductants over alkanes (4, 6), the appreciable SCR activity even of undoped acidic solids (H–ZSM-5, Al_2O_3 (7, 8)), and the deleterious role of Na^+ ions in SCR-HC (reductant methane) over Pd– (9) and Ga–ZSM-5 (10). On this basis, and supported by reports that Cu–ZSM-5 is Brønsted acidic even when overexchanged (11, 12), bifunctional reaction mechanisms have been proposed where (oxidized) carbonaceous deposits, the formation of which would be favored by Brønsted acidity, play a key role as a reductant for NO (or intermediate NO_2) (6, 13–15). On the other hand, there is increasing evidence that Brønsted acidity may not be necessary for SCR-HC at least over Cu–ZSM-5. Such conclusion was arrived at by Jen *et al.* in a study of Cu–ZSM-5 with high Cu/Si or Si/Al ratio (16) and by Centi *et al.*, who compared Cu–ZSM-5 with catalysts in which copper was dispersed in the boralite analog to ZSM-5, which is only mildly Brønsted acidic (17). Indeed, the present discussion of reaction mechanisms is much focused upon proposals explaining the course of the reaction without invoking a relevant function for Brønsted sites (18–27).

Another point of debate is the structure of the active sites in Cu–ZSM-5. SCR-HC was first reported for "overexchanged" Cu–ZSM-5 ($Cu/Al > 0.5$) (1), and an optimum performance of overexchanged samples in series with varying copper content has been reported several times since then (28, 29). The facile interconversion between Cu(II) and Cu(I) in overexchanged Cu–ZSM-5 (30–33) is often considered to be essential for SCR catalysis. It has been attributed to extralattice oxygen (ELO) associated with the excess copper (34–38). Various proposals for

[1] To whom correspondence should be addressed. Fax: +49 234 7094 115. E-mail: w.gruenert@techem.ruhr-uni-bochum.de.

0021-9517/97 $25.00

copper structures bearing the ELO have been put forward: Cu^{2+}–O–Cu^{2+} dimers (34, 35), small zeolite-hosted copper-oxide clusters (36, 37), possibly anchored via copper ions at exchange positions adjacent to only one Al atom (38). On the other hand, *in situ* ESR investigations on working Cu–ZSM-5 of less than 100% Cu^{2+} exchange degree have shown the copper ions exclusively in the +2 state (39), and the SCR activity has been assigned to isolated copper ions for such "underexchanged" Cu–ZSM-5 (39, 40). The relevance of this result is illustrated by an example reported by Ciambelli *et al.* (41) according to which the "normalized" SCR rates (related to the total copper amount) were highest when the exchange degree approached 100% and decreased considerably above, which calls in question the importance of the excess copper.

The present paper reports an attempt to contribute to this discussion by the investigation of Cu–Na–ZSM-5 catalysts that contain the full amount of Na^+ ions of the parent zeolite (42). Such materials should have little chance to preserve Brønsted acidity, and the Cu species, which are in excess of the stoichiometric cation quantity, may be expected to be dispersed on extralattice positions. The preparation technique employs chemical transport phenomena which occur when physical mixtures of Na–ZSM-5 and copper compounds ($CuCl_x$, $Cu(NO_3)_2$, etc.) are heated in inert atmosphere, and they have been reported for many different systems including CuCl/Na–Y by Xie and Tang (43). By using surface-analytical techniques (XPS, X-ray-induced Auger electron spectroscopy (XAES)) we found that $CuCl_2$ becomes reduced to CuCl and spreads out over the external crystallite surface first before entering the zeolite pores at a significantly higher temperature (42). Only Cu(I) entities penetrate into the pore system, which makes the residual oxygen partial pressure in the system a critical parameter for the success of the transport experiment. On the other hand, it was found that not only Cu(I)-chloride species can enter the zeolite cavities, but also Cu(I)-oxide species.

This chemical transport technique should be differentiated from the well-known solid-state ion exchange (SSI (44, 45)). The latter also includes transport phenomena, but is actually a stoichiometric exchange reaction. H- or NH_4-zeolites are used in SSI (with Cu compounds; cf. (46–48)), and the evolution of volatile compounds (HCl, NH_4Cl, H_2O) provides a plausible explanation for the driving force of the transport involved. The driving force for the chemical transport of Cu compounds into Na–ZSM-5 (42) is not clear, and neither is the nature of the resulting material: It may form a nonstoichiometric host–guest system with the copper compound as a guest, or stoichiometrical exchange of Na^+ by Cu^+ may take place rendering a Na compound hosted in the crystallite voids or appearing at the external surface. The latter has been recently reported for the interaction of CuCl with Na–Y by Jiang and Karge (49) and assigned as a special case of solid-state ion exchange. On the other hand, it has been demonstrated that NaCl can be incorporated into Na–Y to produce intrazeolite salt dispersions just by dry heating of mechanical mixtures (50), which is, clearly, an example for a nonstoichiometric host–guest system.

In the following, the catalytic behavior of Cu–Na–ZSM-5 materials prepared by chemical transport in the SCR of NO by propene will be reported and compared with that of reference samples prepared by aqueous exchange. For the characterization of the samples prior to and after catalysis, the surface-analytical techniques used previously (XPS, XAES) have been complemented by IR spectroscopy of adsorbed pyridine, which provides evidence on the Brønsted acidity of the samples and allows copper species dispersed in the bulk of the zeolite crystals to be traced (49). The discussion will cover the role of Brønsted acidity and of the excess copper, with particular attention to the nature of the copper species in Cu–Na–ZSM-5 systems prepared by chemical transport.

METHODS

Materials. The samples employed in this study were prepared from Na–ZSM-5 (Si/Al $\approx$ 13, Chemiewerk Bad Koestritz, Germany) and copper compounds ($Cu(CH_3COO)_2 \cdot H_2O$; $Cu(NO_3)_2 \cdot 3H_2O$, "p.a. grade"; CuCl, "reinst" grade, Merck). Reference samples were prepared by single and fivefold aqueous exchange with copper acetate solutions using the procedures given in (51). The copper content of the reference samples as determined by ICP is reported in Table 1, where the codes r45, r80, and r220 used in this paper to denote these samples are introduced as well. The two samples obtained by fivefold exchange did not contain significant amounts of Na.

Physical mixtures of copper compounds with Na–ZSM-5 were prepared by ball-milling the dried zeolite together with CuCl or with $Cu(NO_3)_2$. These mixtures were subsequently heated in flowing N_2 at 823 K (4 h) and 873 K (8 h), respectively, to effect the transport of the copper species into the zeolite crystal (42) ("$CuCl_x$/Z" and "CuO_x(N)/Z," cf. Table 1). Copper acetate was mixed with Na–ZSM-5 by precipitating it from a solution onto the external zeolite surface ("coating," sample code "Cuac-Z"). This coating was performed in a rotary evaporator by mixing wetted zeolite material with the solution and evaporating the solvent in a few minutes. Such rapid evaporation was essential to obtain a material with copper detectable by XPS/XAES only in extrazeolite location (Auger signal, Fig. 1, spectrum e, for spectral assignment see below). Batches containing copper both in intra- and in extrazeolite locations (cf. Fig. 1, spectrum d) were discarded. With the copper-acetate-coated precursor, the transport experiment was performed at 823 K in flowing He or N_2 (3 h; "CuO_x(ac)/Z"). In one experiment,

TABLE 1

Cu/Si Atomic Ratios in the Surface Layer of Cu–ZSM-5 Catalysts of Different Preparation

Sample (code)	Cu content[a] (wt%)	Exchange degree (%)	Cu/Si atomic ratio By XPS	Cu/Si atomic ratio Bulk
Reference catalysts				
r45	1.6	≈45	0.073	0.015
r80	2.8	≈80	0.15_5	0.027
r220	7.7	≈220	0.26	0.075
Cuac-Z[b]	2.1		0.25–0.70[c]	0.020
CuO_x(ac)/Z[d]	2.1		0.09	0.020
after catalysis	2.1		0.034	0.020
Cuac-Z/H-Z[e], after catalysis	1.05		0.011	0.010
CuO_x(N)/Z[f]	4.2		0.16_5	0.040
$CuCl_x$/Z[g]	5.1		0.17	0.048

[a] For reference catalysts and $CuCl_x$/Z by ICP, for the remaining samples calculated from ingredients of physical mixture.
[b] Cu-acetate-coated Na–ZSM-5, initial.
[c] Different batches.
[d] Cuac-Z after transport experiment.
[e] 1 : 1 mixture Cuac-Z/H–ZSM-5.
[f] $Cu(NO_3)_2$/Na–ZSM-5, after transport experiment.
[g] CuCl/Na–ZSM-5, after transport experiment (involving some CuCl loss).

the Cuac-Z precursor was physically mixed with H–ZSM-5 (CBV 5010, Si/Al ≈ 25, provided by Elf Aquitaine) at a ratio of 1 : 1 by weight prior to the thermal treatment ("Cuac-Z/H-Z").

The catalytic runs were performed with gases supplied by Messer-Griesheim: He 4.6 grade, and prefabricated mixtures, propene (2%)/He, NO (2%)/He, O_2 (20%)/He.

Physicochemical characterization. XPS and X-ray-induced Auger spectra were recorded with a Leybold LH 10 spectrometer equipped with a pretreatment chamber that ensures sample transfer into the vacuum system without contact with the ambient atmosphere. Spectra were excited with Al$K\alpha$ radiation (1486.6 eV, 12 kV · 23 mA) and measured with the analyzer in the pass-energy mode (pass energy 100 eV). Cu 2p, Si 2p, O 1s, Na 1s, and C 1s XPS lines and the CuL3VV Auger signal were recorded, in addition to the N 1s and Cl 2p lines where appropriate. The binding energy (BE) scale was referenced to Si 2p = 102.7 eV, which yielded an average C 1s BE of 284.5 ± 0.2 eV. The CuL3VV kinetic energies (KE) were processed analogously.

The location of the copper species (intra- and extrazeolite) was assessed on the basis of the KE of the CuL3VV Auger line and of the resulting Auger parameter

$$\alpha_{Cu} = \text{BE (Cu } 2p) + \text{KE (Cu}L\text{3VV)}.$$

As differential-charging effects are quite frequent with physical mixtures, BE and KE values reported for such samples should be taken with some caution, and the Auger parameters should be preferred with the copper data as they are not influenced by charging effects.

During data acquisition, we could not always avoid the photoreduction of intrazeolite Cu^{2+} to Cu^+ (33). In the Auger spectra, these states are not easily separated when coexisting. In this paper, attention will be focused on the location of Cu species, which is reflected in shifts of the CuL3VV Auger line far exceeding that between Cu^{2+} and Cu^+ (33, 37, 52). Therefore, Cu 2p XPS spectra will not be shown, while the CuL3VV Auger spectra will be presented, with the Cu 2p BE and the majority species indicated by XPS given in insets. The Auger parameters reported were calculated from the Cu 2p BE of this majority species and the KE at the Auger signal maxima. Due to the strong overlap of the Auger signals of coexisting Cu^{2+} and Cu^+, the Auger parameters cannot always be unambigously attributed to one of these oxidation states, but only to extra- or intrazeolite copper. Atomic ratios for the surface layer were obtained from XPS intensity ratios by using the Scofield sensitivity factors (53) together with an experimentally derived response function of the spectrometer to the variation of the photoelectron KE.

DRIFTS spectra of adsorbed pyridine were measured with a Perkin–Elmer 1710 FTIR spectrometer. Prior to pyridine adsorption, the samples were outgassed in flowing nitrogen (heating up at ≈10 K/min; 15 min (reference samples, 1 h) at 773 K), which results in zeolite dehydration with a concomitant (partial) reduction of Cu^{2+} to Cu^+. After recording of the zeolite spectrum at room temperature, pyridine was adsorbed and the samples were flushed in N_2. With samples containing no Na, this procedure provided quite intense signals of physisorbed pyridine (1441 and 1590–1595 cm^{-1} (55)), which were mostly removed by flushing the samples at 373 K for 15 min. With most of the samples the acquisition of the spectra was very much complicated by a low reflectivity (dark gray material), which resulted in a sometimes quite high noise level in the spectra. All spectra are presented unsmoothed.

Catalysis. The SCR of NO by propene was studied in a microcatalytic flow reactor at reaction temperatures between 873 and 573 K (varied in downward direction). NO conversions were measured with a feed gas containing 1000 ppm NO, 1000 ppm C_3H_6, and 2% O_2 in He at a space velocity of 32,000 vvh. The reaction products were analyzed by a combination of GC and mass-spectrometric analysis. Different catalyst pretreatments were adopted for reference samples and those samples prepared from physical mixtures. The former were treated in He at 823 K for 1 h prior to the catalytic experiment. The latter were treated in He at the temperature used in the original transport experiment (823 or 873 K) for 1 h before the run and each time before a new reaction temperature was established.

RESULTS

Spectroscopic investigation of CuNa–ZSM-5 obtained by chemical transport. Figure 1 shows the Cu*L*3VV Auger spectra of the reference catalysts (a–c), of the initial copper-acetate coated-Na–ZSM-5 (Cuac-Z), where an inacceptable batch (d) is compared with a proper one (e), and of materials prepared from the physical mixtures by chemical transport (f–h, catalyst state prior to catalysis). All samples but the copper-acetate-derived ones (d, e) had been subjected to thermal treatment in inert gas prior to surface analysis (cf. legend to Fig. 1). The majority copper state was Cu^{+} in these cases, which was deduced from a comparison of the spectra at short and at full acquisition time. In the spectra d and e, the majority oxidation state was Cu^{2+}.

The reference catalysts exhibit a Cu*L*3VV Auger signal at a KE of 913–913.5 eV ($\alpha_{Cu} < 1846.5$ eV), which was assigned to intrazeolite copper previously (33, 37). In the spectrum of r220 (c), a second line typical of extrazeolite Cu is present. Similar signals of intra- and extrazeolite copper were observed with Cuac-Z when the coating procedure was extended over a long time (Fig. 1d). Transport experiments were performed only with precursor material exhibiting a single Cu Auger signal (e; cf. Experimental). It should be noted that neither the Cu*L*3VV KE nor the Auger parameter of the copper-acetate precipitate coincide with that of crystalline $Cu(CH_3COO)_2 \cdot H_2O$ (917.8 and 1851.5 eV, respectively). The value of the precipitate (almost 1850 eV) is, however, not in the range typical of intrazeolite locations (cf. Discussion).

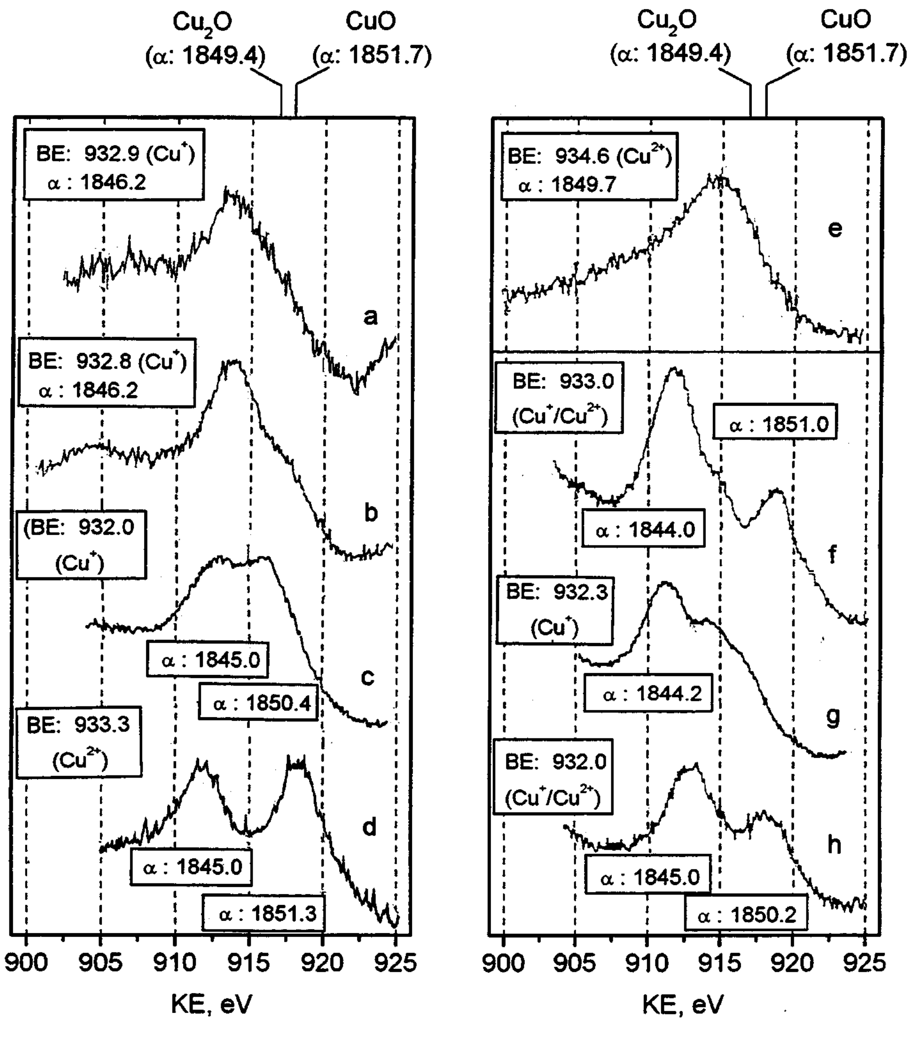

FIG. 1. X-ray induced Auger spectra of Cu–ZSM-5 catalysts. (a–c) Reference samples; pretreatment: air, 673 K, 1 h, then vacuum, 753 K, 1 h; (a) r45; (b) r80; (c) r220. (d, e) Cuac-Z, different batches (acquisition of spectra at 150 K); (d) Cuac-Z, slow solvent evaporation; pretreatment: air, 673 K, 1 h; (e) Cuac-Z, rapid solvent evaporation, no pretreatment. (f–h) Materials prepared by chemical transport: (f), $Cu(NO_3)_2$/Na–ZSM-5, after N_2, 873 K, 8 h ($\Rightarrow$ CuO_x(N)/Z); (g) CuCl/Na–ZSM-5, after vacuum, 823 K, 1 h ($\Rightarrow$ $CuCl_x$/Z); (h) Cuac-Z, after N_2, 823 K, 3 h ($\Rightarrow$ CuO_x(ac)/Z). XPS BE, eV, and Auger parameter α_{Cu}, eV of major Cu state indicated in insets.

The Auger signal of intrazeolite copper appeared in all samples prepared by thermal transport from the physical mixtures (Fig. 1, spectra f–h), but it was always accompanied by a signal of residual extrazeolite copper. After the thermal treatment, neither could acetate carbon be found in the C 1*s* signal of the copper-acetate-derived CuO_x(ac)/Z nor could an N 1*s* line be detected in the spectrum of the copper-nitrate-derived CuO_x(N)/Z. In $CuCl_x$/Z, the Cl/Cu atomic ratio remained almost constant: it decreased slighly from 1.0 in the physical mixture to 0.80 after the transport experiment. A dramatic increase of the Na 1*s* signal intensity was not observed in any sample. With the copper-nitrate- and copper(I)-chloride-based mixtures, the thermal treatment did not affect the Na/Si intensity ratio at all. With Cuac-Z, the latter increased by 35% after the transport experiment; after catalysis, however, the value was 25% below the initial value.

In Table 1, the Cu/Si atomic ratios in the near-surface region as measured by XPS are compared with the bulk Cu/Si ratios. It can be seen that all samples but two are highly surface-enriched in copper. This includes also the reference catalysts, although these had been already subjected to severe thermal treatment (cf. legend to Fig. 1). Hence, even at a bulk exchange degree of only ≈80%, there are overexchanged regions near the external surface. The surface enrichment noticed after the transport experiment is not surprising since XAES reveals the presence of residual extrazeolite Cu in all samples. Notably, with the CuO_x(ac)/Z sample, the Cu/Si ratio seen by XPS approaches the bulk one after catalysis. Both values coincide in the material obtained by thermal treatment of the physical mixture Cuac-Z/H-Z (i.e., after catalysis).

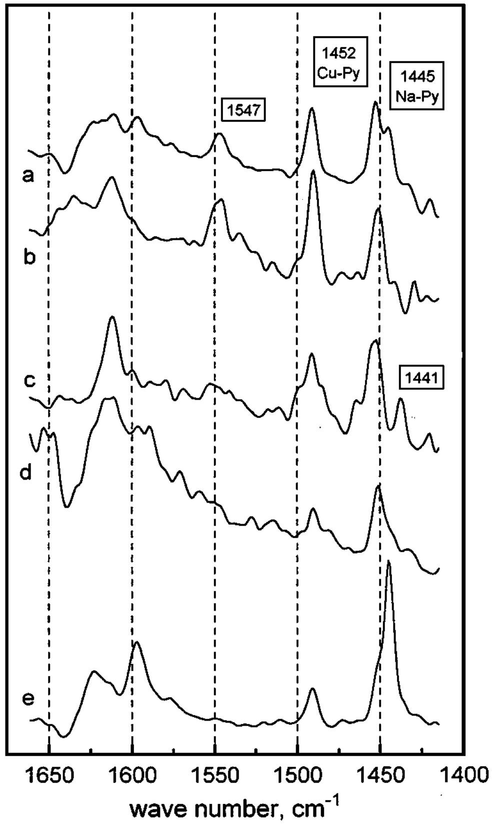

FIG. 2. IR spectra of pyridine adsorbed on Cu–ZSM-5 catalysts (difference spectra). (a–c) Reference samples; pretreatment: air, N_2, 773 K, 1 h; (a) r45; (b) r80; (c) r220 (d, e) materials prepared by chemical transport: (d) $CuCl_x$/Z, (e) CuO_x(N)/Z.

Figure 2 reports the IR spectra of pyridine adsorbed on the reference catalysts (a–c) and on materials obtained by thermal treatment from mixtures of copper-nitrate and Cu(I)-chloride with Na–ZSM-5 (d, e). The purpose of these experiments was to detect Brønsted sites (≈1545 cm^{-1}) as well as to differentiate between Cu and Na sites by examination of the regions around 1450 and 1600 cm^{-1} (12, 49, 55). We will concentrate here on the former region because the noise problem encountered with our dark samples appears to be more serious at the higher frequencies, but it should be noted that the tendencies described are, indeed, parallel in both regions.

In the spectra of the reference samples, bands at 1452 and 1615 cm^{-1} appear. With r45, an additional band is observed at 1445 cm^{-1}, and there is intensity below 1600 cm^{-1}. There are Brønsted sites in the reference samples as revealed by the bands at ≈1545 cm^{-1}. A weak band at 1441 cm^{-1} in spectrum c (r220) is due to a small amount of residual physisorbed pyridine. The spectra of the materials obtained by thermal treatment of physical mixtures differ markedly in the regions around 1450 and 1600 cm^{-1}. With CuO_x(N)/Z (e), the major intensity contributions are below 1450 (1600) cm^{-1}, but there is a shoulder above 1450 cm^{-1} and a distinct band around 1615 cm^{-1}. The opposite is true for $CuCl_x$/Z (d): Here, the major intensity is above 1450 (1600) cm^{-1}. In the former sample, there is no Brønsted acidity, while some noise in the 1550 cm^{-1} region prevents unambigous conclusions on that point for the latter. Other significant features of the spectra are a band at 1650 cm^{-1} in the spectrum of $CuCl_x$/Z (d) and a small band at ≈1580 cm^{-1} in all samples containing Na^+ (spectrum e, cf. also Fig. 5, spectra a and b). The latter is sometimes not resolved from the neighboring absorption at ≈1595 cm^{-1}, which gives rise to an increasing background (spectra a and d, Fig. 5, spectrum c). Both features are also present in the work of Jiang and Karge on the solid-state reaction between Na–Y and CuCl (49). A band in the 1580 cm^{-1} region can be expected for coordinatively bound pyridine (56); hence, the former signal is assigned to pyridine adsorbed on Na^+. The band at ≈1650 cm^{-1} appears in (49) only in the initial spectra, but remains unassigned. As it disappears in the course in the interaction of CuCl with Na–Y, during which the formation of NaCl is observed, it may be due to an interaction of the pyridine with the highly dispersed crystalline CuCl.

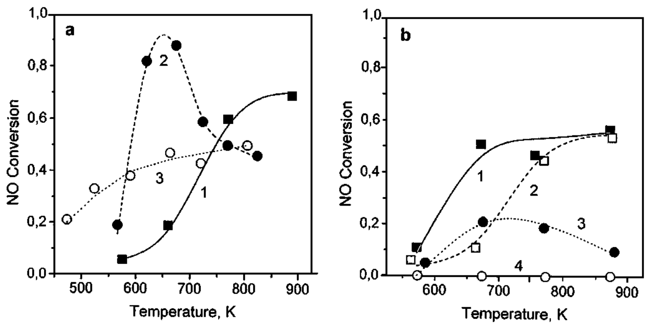

FIG. 3. SCR activity of Cu–ZSM-5 catalysts. 1000 ppm NO, 1000 ppm C_3H_6, 2% O_2 in He, 32,000 vvh. (a) Reference samples; curve 1, r45; curve 2, r80, curve 3, r220. (b) Catalysts prepared by chemical transport; curve 1, CuO_x(ac)/Z; curve 2, Cuac-Z/H-Z; curve 3, $CuCl_x$/Z; curve 4, CuO_x(N)/Z.

Catalytic properties. The catalytic activity of the various Cu–ZSM-5 samples is summarized in Fig. 3 and in Table 2, where the maximum rate of NO conversion is related to the total copper content to yield a normalized reaction rate R_{Cu}. Figure 3 reports the temperature dependence of the NO conversion at 32,000 vvh for the ion-exchanged reference samples (a) and the catalysts prepared by chemical transport (b). With the reference samples, the highest NO conversion was observed with r80; the highest normalized reaction rate, however, was obtained with the underexchanged sample r45 (Table 2). The temperature dependence of the NO conversion exhibits marked differences between all three reference catalysts. With r220, despite a low general activity level, an NO conversion of 20% was obtained even at 473 K where other Cu–ZSM-5 catalysts are far from being active. At the same time, the propene conversion to carbon oxides was almost complete with this catalyst. With r80, a steep increase of the NO conversion was found between 573 and 623 K with the conversion peaking below 670 K, which is typical for slightly overexchanged samples (37). With r45, the activity increased more gradually and at higher temperatures, no activity maximum could be discerned below 870 K.

TABLE 2

Reaction Rates of the SCR of NO by Propene over Cu–ZSM-5 Catalysts (Normalized to the Total Copper Content)

Sample (code)	$R_{Cu}{}^{a}$ (min^{-1})	T (max) (K)
r45	0.20	873
r80	0.14_5	673
r220	0.03	873
CuO_x(N)/Z	0	—
$CuCl_x$/Z	0.02	673
CuO_x(ac)/Z	0.10–0.13[b]	873
Cuac-Z/H-Z	0.24	873

[a] r (NO conversion)/(n(Cu)/g cat.) at rate maximum.
[b] Strongly dependent on batch of initial Cuac-Z; lowest value observed, 0.05 min^{-1}.

Significant differences are also visible in the catalytic behavior of the samples prepared by chemical transport (Fig. 3b). CuO_x(N)/Z does not exhibit NO reduction activity at all; it catalyzes, however, the total oxidation of propene. On the other hand, NO conversions of >50% are obtained with CuO_x(ac)/Z, where the lower limit of the useful temperature region is similar as in the case of r80. Due to the lower Cu content, the maximum R_{Cu} measured with CuO_x(ac)/Z is on the same order of magnitude as that with the latter reference sample (Table 2). It shall not be withheld that the SCR activity of CuO_x(ac)/Z may vary considerably between different batches of the Cuac-Z precursor (cf. footnote 2 in Table 2). Normalized reaction rates R_{Cu} of 0.10–0.13 min^{-1} have been, however, repeatedly measured with this type of material.

When the Cuac-Z precursor is mixed with an equal portion of H-ZSM-5, the resulting Cuac-Z/H-Z mixture provides the highest normalized reaction rate measured in this study. The temperature dependence of the SCR activity (Fig. 3b) is quite different from that in absence of H–ZSM-5 and resembles that of r45. The NO conversion increases gradually between 670 and 770 K to reach its highest value at 870 K. This shift of the useful temperature interval to higher temperatures for a physical mixture of a precipitated Cu–ZSM-5 with H-ZSM-5 has been reported before (37). The chlorine-containing $CuCl_x$/Z possesses also some SCR activity.

Postcatalytic spectroscopic investigations. Figures 4 and 5 report some postcatalytic studies of the copper location and the acidic properties of the more relevant samples. In Fig. 5, the CuL3VV Auger spectra of the Cu-acetate-derived samples (without and with H–ZSM-5 admixed, spectra b and c) are compared with that of CuO_x(N)/Z (a). In the latter case, the majority Auger signal is clearly that of extrazeolite copper. In both Cu-acetate-derived catalysts, however, the low-KE signal resulting in $\alpha_{Cu} = 1847.3$ eV predominates. This value is higher than those usually found for intrazeolite copper (see Fig. 1). This may be partly due to inaccuracies in the determination of the line positions, as the intensity of the copper signals is very low in these samples and the signals appear on a curved background. In the case of CuO_x(ac)/Z (b), however, a signal of extrazeolite Cu ($\alpha_{Cu} = 1849.9$ eV) is clearly visible, so there remains little doubt that the main signal ($\alpha_{Cu} = 1847.3$ eV) arises from intrazeolite Cu species.

In Fig. 5, IR spectra of pyridine adsorbed onto the most active catalysts obtained by chemical transport are given. Curve a shows the spectrum of the initial Cuac-Z for comparison. It is dominated by signals at 1445 and 1598 cm^{-1}; the 1545 cm^{-1} region is almost flat. Spectrum b refers to the state of CuO_x(ac)/Z after catalysis: The strong band of the Na–Py complexes (1445 cm^{-1}) is now significantly broadened by a shoulder extending above 1450 cm^{-1}, and

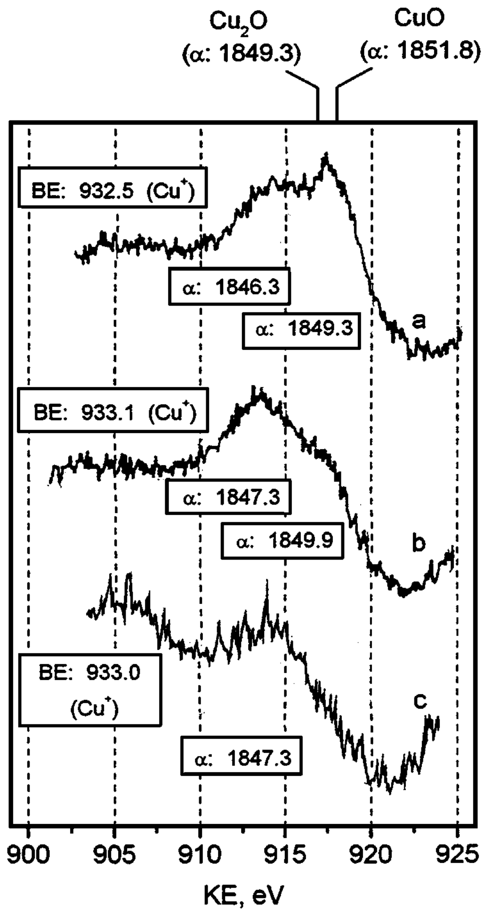

FIG. 4. X-ray-induced Auger spectra of Cu–ZSM-5 catalysts prepared by chemical transport, after use in catalysis. (a) CuO_x(N)/Z; (b) CuO_x(ac)/Z; (c) Cuac-Z/H-Z. XPS BE, eV, and Auger parameter α_{Cu}, eV of major Cu state indicated in insets.

the intensity above 1600 cm^{-1} has increased as well. As expected, the sample does not exhibit Brønsted acidity. For the physical mixture of Cuac-Z with H–ZSM-5 (Cuac-Z/H-Z), it was not possible to obtain a meaningful spectrum for the initial state: The dehydration procedure necessary before the adsorption of pyridine, though performed at the rather low temperature of 623 K, already initiated some mobility of the copper: The resulting spectrum was different from the expected superposition of signals from Cuac-Z (spectrum a) and H–ZSM-5. Spectrum c refers to the state of this mixture after catalysis. There are well-separated bands below and above 1450 (1600) cm^{-1}. In the 1545-cm^{-1} region, there is no signal beyond the unfortunately rather high noise level; i.e., the admixed H–ZSM-5 has not preserved its Brønsted acidity.

DISCUSSION

In the following, the spectroscopic evidence obtained will be summarized to describe the structure of Cu–Na–ZSM-5 catalysts prepared by chemical transport. Subsequently, the catalytic results will be related to the structural properties to derive conclusions about the relevance of Brønsted acidity and excess copper in the SCR of NO by propene over Cu–ZSM-5.

Distribution and structure of intrazeolite copper. While techniques involving chemical transport are well recognized in the preparation of supported oxide catalysts (e.g., MoO_3/Al_2O_3, V_2O_5/Al_2O_3 (43)), there are only a few reports about the application of such techniques for the introduction of transition-metal compounds into zeolites (43, 50, 57). For Cu/zeolite systems, the combination of XPS and XAES is a powerful means to study the success of the transport experiment because the L3VV Auger line of intrazeolite Cu is shifted strongly compared to that of Cu in its bulk oxides (33, 37, 52). This is illustrated in Fig. 1 in the spectra of the reference samples (spectra a–c) and of the initial Cu-acetate-coated Na–ZSM-5 (d, e), where the potential of the technique to differentiate coexisting intra- and extrazeolite copper becomes evident (cf. spectra c and d).

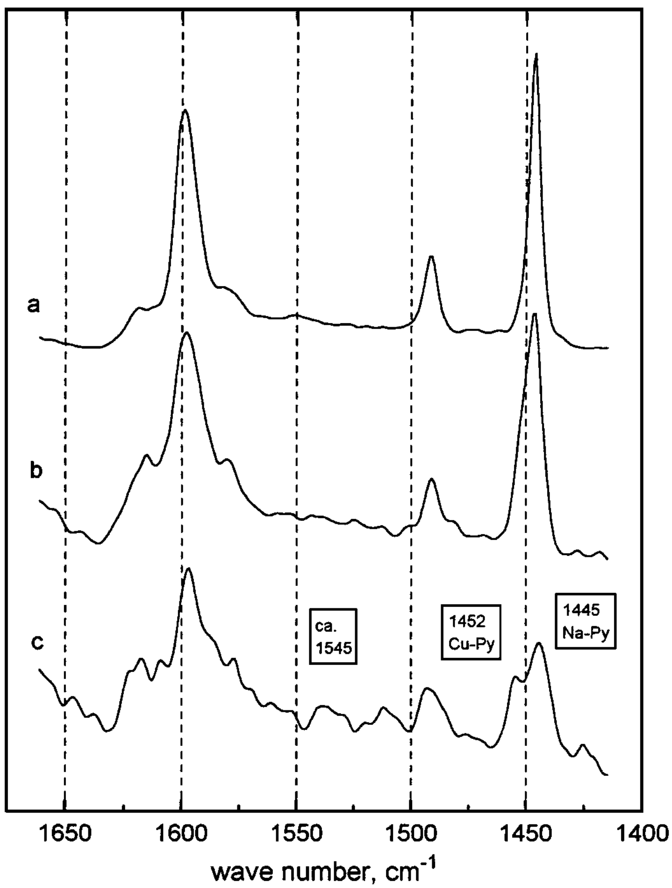

FIG. 5. IR spectra of pyridine adsorbed on Cu–ZSM-5 catalysts derived fron Cuac-Z (difference spectra). Samples dehydrated at $T_d = 773$ K for 15 min. (a) Cuac-Z; (b) CuO_x(ac)/Z after catalysis; (c) Cuac-Z/H-Z after catalysis.

The Auger parameters α_{Cu} of these copper states differ by several electron volts.

The high Cu$L3VV$ Auger-line shift, which leads to a change of the Auger parameter, should be attributed to final-state effects; its actual origin is, however, not clear. In our opinion, it is due to the difference between final states, the wave function of which involves extended states (i.e., a valence band as in crystalline copper oxides) or localized orbitals (i.e., oxygen ligands in environments of low point and translational symmetry as on zeolite sites). Such shifts of Auger line and Auger parameter should, therefore, arise not only for isolated Cu at cationic sites, but may originate from any Cu aggregate too small or too irregular to possess a valence band (e.g., small intrazeolite copper oxide clusters as detected in Cu–ZSM-5 by EXAFS (37)). From this viewpoint, the magnitude of the shift may depend on the nuclearity and the coordination geometry of the copper entity detected. Indeed, in the present study, the Auger parameters of samples containing intrazeolite Cu predominantly in the +1 state vary in a rather broad range (1844.0–1847.3 eV, cf. Figs. 1 and 4). The decrease of α_{Cu} of $Cu(CH_3COO)_2$ upon precipitation as a deposit of (presumably) poor crystallinity (Fig. 1, spectrum e) may be understood on the same basis. It should be noted, however, that this interpretation of a proven and useful experimental effect has yet to be substantiated by more detailed investigations.

The chemical transport of Cu_xCl_y and Cu_xO_y species into the zeolite from mixtures of $CuCl_2$, CuCl, or $Cu(NO_3)_2$ with Na–ZSM-5 has been studied in detail by XPS/XAES recently (42), and the migration of both Cu(I)-chloride and -oxide species has been demonstrated from the spectra of Cu and of the remaining elements (Cl, C, N). Spectra g–h in Fig. 1 resume the final results for CuCl/Na–ZSM-5 and $Cu(NO_3)_2$/Na–ZSM-5 and add the same for Cu-acetate-coated Na–ZSM-5, where the presence of intrazeolite copper is also evident. Almost all samples are highly surface-enriched in copper (Table 1) and contain some extrazeolite copper in addition to the intrazeolite species (Fig. 1). However, the surface-analytical techniques, do not supply information about the depth of migration and the amount of Cu penetrated into the zeolite voids because the deeper layers are not accessible to these methods and an assessment of the amount of extrazeolite copper would require information about its aggregate size.

The penetration depth of the Cu species can be assessed on a qualitative level from IR spectra of adsorbed pyridine because the signals of the ring vibrations at approximately 1450 and 1600 cm^{-1} differ significantly between molecules coordinated to Na^+ and Cu^{n+} (12, 49, 55) ($n = 1$, possibly).[2] This is well illustrated by a comparison of the spectra recorded with the reference samples r45, r80, or r220 (Fig. 2, curves a-c) and with the initial Cuac-Z (Fig. 5, curve a). In the former, the signals of the Cu–Py complex (1452/1615 cm^{-1}) are well visible (in the spectrum of r45 together with a contribution of Na–Py at 1445/1598 cm^{-1}). In Cuac-Z, there is practically no intensity above 1450 (around 1615) cm^{-1} because the copper, though well spread over the external crystallite surface (cf. Table 1), is of much lower dispersion than any of the intrazeolite species (Na or Cu ions) in the reference catalysts. Thus, the appearance of intensity above 1450 cm^{-1} (around 1615 cm^{-1}) should indicate the penetration of copper into the zeolite crystal as there is no other way to obtain an amount of Cu adsorption sites comparable to that of the Na sites.

On this basis, spectra d and e in Fig. 2 reveal an important difference in the transport behavior of Cu(I) associated with chlorine or with oxygen. In CuO_x(N)/Z (e), a distinct but weak shoulder due to Cu–Py may be discerned at the high-energy side of the Na–Py band at 1445 cm^{-1}. Spectrum d measured with $CuCl_x$/Z, however, is dominated by the Cu–Py bands at 1452 and 1615 cm^{-1}, while the 1445-cm^{-1} band has almost vanished. It should be noted that the Auger spectra of these two samples (Fig. 1, curves f and g) are rather similar, indicating the presence of intrazeolite copper. The IR spectra suggest that the copper penetrates deeper into the crystallites when associated with chlorine than with oxygen as would be expected from the volatility of the corresponding bulk compounds. The same trends have been also observed in the stoichoimetric solid-state ion exchange of copper chlorides and oxides with H zeolites (46–48).

The problem if the transport of the Cu entities into the zeolite is coupled with a stoichiometric exchange $Cu^+ \rightarrow Na^+$ (solid-state ion exchange, cf. (49)) or leads to the intercalation of the Cu compounds in the zeolite voids (nonstoichiometrical host–guest system, in analogy to (50)), may be approached by tracing Na compounds that may have been formed during the transport experiment.

In our CuCl/Na–ZSM-5 system, we did not find either XRD lines of NaCl or an enrichment of Na near the external crystallite surface, which could have indicated the formation of extrazeolite NaCl either in low (XRD) or in high (XPS) dispersion. In $CuCl_x$/Z, the Na Auger parameter ($\alpha_{Na} = \mathrm{BE}$ (Na 1s) + KE (Na KLL)) was 2060.5 eV. This is slightly below the values found in an earlier investigation of Na–ZSM-5 ($\alpha_{Na} = 2061.1$ eV (58)), but very close to the limits of Na Auger parameters reported for a variety of zeolite materials (2060.6–2061.1 eV (58, 59)). In NaCl, α_{Na} is reported to be 2061.9 eV (59), i.e., much higher than in $CuCl_x$/Z. No shoulders were observed at the Na XPS and Auger signals that could have indicated NaCl even as a minority species. Taken together, these results exclude the formation of extrazeolite NaCl in our samples. However, they do not completely exclude an *intrazeolite* ion

[2] We could not observe a significant difference in the spectra of r45 treated at 823 K in air or in N_2 to obtain the copper predominantly in the +2 and +1 form.

exchange resulting in intrazeolite NaCl clusters, because the Auger parameter of Na in highly dispersed NaCl might differ from that in the bulk compound.

More evidence for the presence of clusters may be sought in the IR spectra. In $CuCl_x$/Z, we found a band at $\approx$1650 cm^{-1} after the transport experiment (Fig. 2, spectrum d), which Jiang and Karge (49) saw only in the initial stages of their solid-state reaction between Na–Y and CuCl. In our initial CuCl/Na–ZSM-5 mixture, which contained CuCl in low dispersion, this band was present in low intensity (spectrum not shown). However, even if this band can be assigned to an interaction of pyridine with the surface of aggregated CuCl, it is no proof for the existence of zeolite-hosted Cu_xCl_y as it may originate also from remaining extrazeolite CuCl portions. The low intensity of the Na–Py contribution to the band around 1450 cm^{-1} (below 1600 cm^{-1}) despite the presence of the full amount of Na ions may be another indication for the existence of intrazeolite clusters covering part of the Na^+ ions. This point must be elucidated in future work.

With the CuO_x/Z materials, the formation of extrazeolite Na compounds was also not indicated by either surface enrichment of Na or shifts of the Na Auger parameter after the treatments were applied to initiate the transport (copper-acetate-coated Na–ZSM-5: $\alpha_{Na} = 2060.6 \pm 0.1$ eV before and after thermal treatment). Interestingly, for one of the initial physical mixtures, the formation of an extrazeolite bulk compound was, indeed, suggested by the Na XPS signal (Na 1*s*, Fig. 6): In the $Cu(NO_3)_2$/Na–ZSM-5 mixture prepared by ball-milling (Cu spectra shown in (42)), a signal with a BE $<$ 1070 eV appeared as a shoulder at the Na 1*s* line (spectrum a). This BE is far below the BE of any known Na compound and arises most likely from a differentially charged phase. It has been demonstrated in Ref. (42) that ball-milling the $Cu(NO_3)_2$/Na–ZSM-5 mixture leads to effective spreading of the copper compound over the external zeolite surface and the loss of the $Cu(NO_3)_2$ signature in XRD. We guess, therefore, that the compound detected by the shoulder below 1070 eV may be $NaNO_3$. Notably, this shoulder disappeared when the mixture was heated (spectrum b). While this may indicate that the exchange of zeolite Na^+ by Cu^+ is unfavorable just at higher temperatures, it is, again, no definite proof for the absence of such an exchange inside the zeolite cavities.

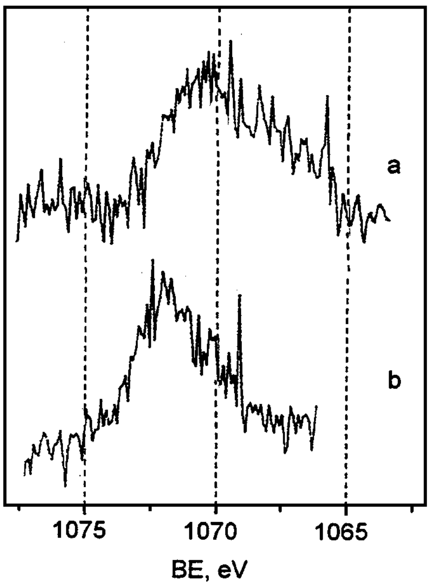

FIG. 6. Evolution of Na 1*s* lineshapes in the preparation of CuO_x(N)/Z. (a) Physical mixture after ball-milling; (b) (a) after N_2, 673 K, 24 h (analogous for treatments at higher temperatures).

Hence, it may be stated that our spectroscopic evidence excludes the formation of Na compounds at the external zeolite surface during the transport treatment. It suggests that an ion exchange $Cu^+ \rightarrow Na^+$ does not occur subsequent to the penetration of Cu compounds into the ZSM-5 crystal whithout, however, definitly exluding such possibility.

The postcatalytic IR spectra of adsorbed pyridine (Fig. 5) show that CuO_x(ac)/Z does not possess Brønsted acidity (spectrum b). If the acetate-coated Na–ZSM-5 (Cuac-Z) was mixed with H–ZSM-5 prior to thermal treatment, the result was, again, the formation of intrazeolite copper (curves c in Figs. 4 and 5). In the resulting material, however, the Brønsted sites of the admixed H–ZSM-5 can no longer be detected. Obviously, if both H–ZSM-5 and Na–ZSM-5 are offered to the copper compound, stoichiometric solid-state ion exchange into the former predominates over the chemical transport into the latter. This is quite plausible because the reaction of copper-acetate with H–ZSM-5 is driven by the evolution of volatile compounds, most likely H_2O and CO_2. The resulting material was no longer surface-enriched in copper (Table 1), and on the basis of our spectroscopic results we describe it as a mixture of a stoichiometrically exchanged Cu–ZSM-5 (exchange degree near 100%) with Na–ZSM-5.

SCR activity and catalyst structure. The catalytic experiments show that copper introduced into Na–ZSM-5 by chemical transport exhibits activity for the SCR of NO by propene. This applies to the chlorine-containing sample $CuCl_x$/Z as well as to chlorine-free catalysts obtained from Cuac-Z. With the latter, the normalized reaction rates R_{Cu} are quite comparable with those of the reference catalysts (Table 2: compare CuO_x(ac)/Z with r80, Cuac-Z/HZ with r45). As the Brønsted acidity of these copper-acetate-derived systems was far below the level seen with the reference catalysts (if not absent at all), Brønsted acidity does not play an essential role in the SCR of NO by propene over Cu–ZSM-5.

This conclusion seems at variance with the work of several groups, which demonstrated the role of zeolite Brønsted acidity with a variety of catalysts active for the

SCR of NO with methane (9, 10) or with copper catalysts used for the SCR of NO with decane (60). Our conclusion relates primarily to the Cu–ZSM-5 system and the reductant propene, and it is well conceivable that different mechanisms are operative with different catalysts and reductants. The NO oxidation activity of H–ZSM-5 (13), for instance, may be an essential ingredient in systems where this function is not well fulfilled by the dopant introduced as an active component. When long-chain alkanes are used (60), the cracking activity supplied by acidic sites may be favorable because the superiority of alkenes over alkanes as reducing agents in the SCR is well known. In addition, Brønsted sites may have a beneficial influence in systems where the active catalyst component tends to aggregate. Such aggregation should be suppressed in Brønsted-acid environments as it is the reverse of solid-state ion exchange which is knwon to be favored in many systems at elevated temperatures.

On this background, there still remain some unexpected features in our results, which will be covered in the following discussion of the catalytic relevance of Cu species—the complete failure of CuO_x(N)/Z and the influence of H–ZSM-5 admixed to the copper-acetete-derived catalyst on the temperature dependence of the catalytic activity.

The postcatalytic Auger electron spectra reveal that in CuO_x(N)/Z, the copper is mostly extrazeolite after catalysis (Fig. 4, curve a), while in CuO_x(ac)/Z, the spectrum is dominated by a signal of intrazeolite Cu (b). The presence of intrazeolite copper in CuO_x(ac)/Z is also confirmed by the postcatalytic IR spectrum of adsorbed pyridine (Fig. 5, curve b) where the strong asymmetry of the main signal (Na–Py) toward wavenumbers above 1450 cm^{-1} (Cu–Py) is evident. While this confirms the well-known fact that extreme small copper aggregate sizes (as provided by the dispersion in a zeolite matrix) are required for rendering the Cu sites selective, it remains to be discussed why the copper location is completely different CuO_x(N)/Z and CuO_x(ac)/Z under the conditions of catalysis. We believe that this is due to a different penetration depth of the Cu_xO_y entities during the transport experiment. In our previous work, we found that reoxidation of Cu–Na–ZSM-5 prepared by chemical transport causes some of the overstoichiometric copper to return to the external surface (42). The segregation was not complete under the conditions applied in Ref. (42) (air, 673 K, 1 h); it may, however, have come to completion with the CuO_x(N)/Z sample under the more severe conditions of catalysis (2% O_2, starting at 873 K) applied in this study. In CuO_x(ac)/Z, the acetate ions present in the physical mixture probably assist the reduction of Cu(II) to Cu(I) during the transport experiment. As the transport phenomena occur only with Cu(I), it is reasonable to assume that the penetration depth obtained with the copper-acetate precursor will exceed that in the copper-nitrate system. Upon reoxidation to Cu(II), part of the copper is then trapped in the zeolite and remains selective in the SCR reaction.

It was an aim of the present study to describe the catalytic function of excess copper introduced into Na–ZSM-5 by a dry technique. The answer depends crucial on the Cu speciation in these systems (Cu exchanged into cation sites or Cu compounds hosted in the zeolite voids), and it has been mentioned above that our spectroscopical evidence favors the nonstoichiometric host–guest structure without definitely excluding the possibility of exchange. There are, however, some tendencies in our catalytic data, which further support the host–guest structure of Cu–Na–ZSM-5 prepared by chemical transport and indicate that zeolite-hosted copper-oxide clusters contribute to the SCR activity of overexchanged Cu–ZSM-5.

Close inspection of the temperature dependence of the SCR activity measured with the reference samples (Fig. 3a) suggests that different copper species catalyze the reaction at different temperatures. Isolated Cu species, which should be the majority species in r45, become active at rather high temperatures, but they provide the highest normalized reaction rates. As mentioned above, the material formed by thermal treatment of the Cuac-Z/H-Z mixture contains the copper isolated as well. Indeed, its catalytic behavior (Fig. 3b) is much reminiscent of that of r45.

Intrazeolite copper oxide clusters as detected by EXAFS in slightly overexchanged Cu–ZSM-5 catalysts (37) may be responsible for the shift of the useful temperature region to lower temperatures. Our r80 sample is not overexchanged from the bulk stoichiometry, but overexchange has been demonstrated for the external region of the zeolite crystals. The SCR activity of r80 and its temperature dependence (Fig. 3a) is close to the behavior known for overexchanged catalysts from the literature (e.g., (37)). The shift of the useful temperature region to lower temperatures goes on with r220, which exhibited some NO reduction activity already at 473 K. The low level of this activity may be due to the extrazeolite copper present in this material, which competes for the reductant propene with its total oxidation activity.

In the systems prepared by chemical transport of copper into Na–ZSM-5, the useful temperature region clearly begins at lower temperatures than with the samples containing copper presumably in isolated form. Notably, the copper content of CuO_x(ac)/Z corresponds to a formal exchange degree of only 60%. If the copper of this catalyst were exchanged into cation sites, the temperature dependence of the SCR activity would be expected to resemble that of r45 and Cuac-Z/H-Z. Moreover, a higher activity should be expected for the copper-chloride derived $CuCl_x$/Z as the $CuCl_x$ entities penetrate much better into the zeolite and should provide a higher exchange degree. What we see, however, is that the SCR activity of CuO_x(ac)/Z becomes appreciable already in a temperature region where the activity of isolated copper is still low (Fig. 3b), and that the

SCR activity of $CuCl_x/Z$ is inferior (cf. also Table 2). This is best explained by assuming a host–guest character of our Cu–Na–ZSM-5 systems, with zeolite-hosted copper-oxide clusters being better active species than copper-chloride clusters and providing activity at lower temperatures than isolated copper ions do.

CONCLUSIONS

Cu–Na–ZSM-5 catalysts were prepared by chemical transport of copper (I) chloride and oxide species into Na–ZSM-5. The formation of intrazeolite copper species was monitored by surface-analytical techniques (XPS, XAES) and by IR spectroscopy (pyridine adsorption). It was found that copper migrates most easily if associated with chlorine. With Cu(II) compounds not containing chlorine, oxidizable anions (acetate) appear to promote the transport phenomenon. In the presence of H–ZSM-5, solid-state ion exchange into the latter is preferred over the migration into the Na-zeolite.

The SCR activity of intrazeolite copper in Cu–Na–ZSM-5 catalysts prepared by chemical transport, and also by solid-state ion exchange, was on the same order of magnitude as with samples obtained by aqueous ion exchange. As the former did not possess Brønsted acidity, the Brønsted sites of the latter are irrelvent for the SCR reaction. Surface-analytical results and specific differences in the temperature dependence of the SCR activity imply that the copper introduced by nonstoichiometrial chemical transport remains as a guest in the zeolite cavities, and that zeolite-hosted copper-oxide clusters contribute to the SCR-activity of overexchanged Cu–ZSM-5 catalysts.

ACKNOWLEDGMENTS

Thanks are due to Mrs. C. Clees and Mr. D. Rutenbeck who performed most of the XPS/XAES measurements and to Mrs. A. Gomann for IR measurements. Financial support by the Fonds der Chemischen Industrie is gratefully acknowledged.

REFERENCES

1. Iwamoto, M., Yahiro, H., Shundo, S., Yu-u, Y., and Mizuno, N., *Shokubai* **32**, 430 (1990).
2. Held, W., König, A., Richter, T., and Puppe, L., *SAE-Paper* 900496 (1990).
3. Iwamoto, M., *Stud. Surf. Sci. Catal.* **84**, 1395 (1994).
4. Shelef, M., *Chem. Rev.* **95**, 209 (1995).
5. Grünert, W., Papp, H., Rottländer, C., and Baerns, M., *Chem. Tech. (Leipzig)* **47**, 205 (1996).
6. Walker, A. P., *Catal. Today* **26**, 107 (1995).
7. Hamada, H., Kintaichi, Y., Sasaki, M., Ito, T., and Tabata, M., *Appl. Catal.* **64**, 1 (1990).
8. Kintaichi, Y., Hamada, H., Tabata, M., Sasaki, M., and Ito, T., *Catal. Lett.* **6**, 239 (1990).
9. Loughran, C. J., and Resasco, D. E., *Appl. Catal.* **B7**, 113 (1995).
10. Kikuchi, E., and Yogo, K., *Catal. Today* **22**, 73 (1994).
11. Matsumoto, S., Yokota, K., Doi, H., Kimura, M., Sekizawa, K., and Kasahara, S., *Catal. Today* **22**, 127 (1994).
12. Connerton, J., Joyner, R. W., and Padley, M. B., *J. Chem. Soc. Faraday Trans.* **91**, 1841 (1995).
13. Hamada, H., Kintaichi, Y., Sasaki, M., Ito, T., and Tabata, M., *Appl. Catal.* **70**, L15 (1991).
14. Petunchi, J. O., Sill, G. O., and Hall, W. K., *Appl. Catal.* **B2**, 303 (1993).
15. Ansell, G. P., Diwell, A. F., Golunski, S. E., Hayes, J. W., Rajaram, R. R., Truex, T. J., and Walker, A. P., *Appl. Catal.* **B2**, 81 (1993).
16. Jen, H. W., McCabe, R. W., Gorte, R. J., and Parillo, D. J., *Prepr. Div. Petrol. Chem. Am. Chem. Soc.* **39**, 104 (1994).
17. Centi, G., Perathoner, S., and Dall'Olio, L., *Appl. Catal.* **B4**, L271 (1995).
18. Obuchi, A., Obi, A., Nakamura, M., Ogata, A., Mizuno, K., and Obuchi, H., *Appl. Catal.* **B2**, 71 (1992).
19. Burch, R., and Millington, P. J., *Appl. Catal.* **B2**, 101 (1993).
20. Shelef, M., Montreuil, C. N., and Jen, H. W., *Catal. Lett.* **26**, 277 (1994).
21. Yokoyama, C., and Misono, M., *Catal. Today* **22**, 59 (1994).
22. Smits, R. H. H., and Iwasawa, Y., *Appl. Catal.* **B6**, L201 (1995).
23. Hayes, N. W., Joyner, R. W., and Shpiro, E. S., *Appl. Catal.* **B8**, 343 (1996).
24. Iwamoto, M., and Takeda, H., *Catal. Today* **27**, 71 (1996).
25. Beutel, T., Adelman, B. J., Lei, G. D., and Sachtler, W. M. H., *Catal. Lett.* **32**, 83 (1995).
26. Lukyanov, D. B., d'Itri, J. L., Sill, G., and Hall, W. K., *Stud. Surf. Sci. Catal.* **101**, 651 (1996).
27. Aylor, A. W., Lobree, L. J., Reimer, J. A., and Bell, A. T., *Stud. Surf. Sci. Catal.* **101**, 661 (1996).
28. Kharas, K. C. C., *Appl. Catal.* **B2**, 207 (1993).
29. Ciambelli, P., Corbo, P., Gambino, M., Minelli, G., Moretti, G., and Porta, P., *Catal. Today* **26**, 33 (1995).
30. Li, L., and Hall, W. K., *J. Catal.* **129**, 202 (1991).
31. Valyon, J., and Hall, W. K., *J. Phys. Chem.* **97**, 1204 (1993).
32. Giamello, E., Murphy, D., Magnacca, G., Morterra, C., Shioya, Y., Nomura, T., and Anpo, M., *J. Catal.* **136**, 510 (1992).
33. Shpiro, E. S., Grünert, W., Joyner, R. W., and Baeva, G. N., *Catal. Lett.* **24**, 159 (1994).
34. Iwamoto, M., Yahiro, H., Mizuno, N., Zhang, W.-Z., Mine, Y., Furukawa, H., and Kagawa, S., *J. Phys. Chem.* **96**, 9360 (1992).
35. Sarkany, J., d'Itri, J. L., and Sachtler, W. M. H., *Catal. Lett.* **16**, 241 (1992).
36. Valyon, J., and Hall, W. K., *Catal. Lett.* **19**, 109 (1993).
37. Grünert, W., Hayes, N. W., Joyner, R. W., Shpiro, E. S., Siddiqui, M. R. H., and Baeva, G. N., *J. Phys. Chem.* **98**, 10832 (1994).
38. Wichterlová, B., Dedecek, J., and Tvaruzkova, Z., *Stud. Surf. Sci. Catal.* **84**, 1555 (1994).
39. Kucherov, A. V., Gerlock, J. L., Jen, H. W., and Shelef, M., *J. Catal.* **152**, 63 (1995).
40. Wichterlová, B., Sobalík, Z., and Vondrová, *Catal. Today* **29**, 149 (1996).
41. Ciambelli, P., Corbo, P., Gambino, M., Indovina, V., Moretti, G., and Campa, M. C., *Stud. Surf. Sci. Catal.* **96**, 605 (1995).
42. Grünert, W., Liese, T., and Schobel, C., *Stud. Surf. Sci. Catal.* **105**, 1517 (1997).
43. Xie, Y.-X., and Tang, Y.-Q., *Adv. Catal.* **37**, 1 (1990).
44. Karge, H. G., and Beyer, H. K., *Stud. Surf. Sci. Catal.* **69**, 43 (1991).
45. Karge, H. G., *Stud. Surf. Sci. Catal.* **105**, 1901 (1997).
46. Kucherov, A. V., Slinkin, A. A., Kondratev, D. A., Bondarenko, T. N., Rubinstein, A. M., and Minachev, Kh. M., *Zeolites* **5**, 320 (1985).
47. Wichterlova, B., Beran, S., Bednarova, S., Nedomova, K., Dudikova, L., and Jiru, P., *Stud. Surf. Sci. Catal.* **37**, 199 (1988).
48. Karge, H. G., Wichterlova, B., and Beyer, H. K., *J. Chem. Soc. Faraday Trans.* **88**, 1345 (1992).

49. Jiang, M., and Karge, H. G., *J. Chem. Soc. Faraday Trans.* **91**, 1845 (1995).
50. Tracht, U., Seidel, A., and Boddenberg, B., *Stud. Surf. Sci. Catal.* **105**, 525 (1997).
51. Iwamoto, M., Yahiro, H., Mine, Y., and Kagawa, S. *Chem. Lett.* 213 (1989).
52. Sexton, B. A., Smith, T. D., and Sanders, J. V., *J. Electron Spectrosc. Relat. Phenom.* **35**, 27 (1985).
53. Scofield, J. H., *J. Electron Spectrosc. Relat. Phenom.* **8**, 129 (1976).
54. Ghosh, A. K., and Curthoys, G., *J. Chem. Soc. Faraday Trans. 1* **80**, 805 (1984).
55. Martin, C., Martin, I., del Moral, C., and Rives, V., *J. Catal.* **146**, 415 (1994).
56. Parry, E. P., *J. Catal.* **2**, 371 (1963).
57. Qiu, S., Ohnishi, R., and Ichikawa, M., *J. Phys. Chem.* **98**, 2719 (1994).
58. Grünert, W., Muhler, M., Schröder, K.-P., Sauer, J., and Schlögl, R., *J. Phys. Chem.* **98**, 10920 (1994).
59. Wagner, C. D., *in* "Practical Surface Analysis" (D. Briggs and M. P. Seah, Eds.), 2nd ed., Appendix 5. Wiley, New York, 1990.
60. Delahay, G., Coq, B., Ensuque, E., and Figueras, F., *Catal. Lett.* **39**, 105 (1996).